Orbital
The electronic journal of chemistry

the electronic journal of chemistry

Full Paper | http://dx.doi.org/10.17807/orbital.v13i5.1625

Computational Chemistry: Sulfamic Acid Catalyzed PEG-400 Mediated Synthesis, Molecular Structure, HOMO–LUMO, UV-visible, Vibrational, and Reactivity Descriptors Analysis of 2-(Furan-2-yl)-1*H*-benzo[*d*]imidazole

Vishnu A. Adole * [a], Bapu S. Jagdale [a], and Ravindra H. Waghchaure [b]

2-(Furan-2-yl)-1*H*-benzo[*d*]imidazole (2-FBI) is synthesized and investigated using computational chemistry in the present analysis. PEG-400 and catalytic amount of sulfamic acid presents green protocol for the synthesis of 2-FBI. FT-IR, ^{1}H NMR, and ^{13}C NMR spectroscopic methods were used to characterize the structure of 2-FBI. The density functional theory (DFT) approach was used to perform the theoretical calculations, with a basis set of 6-311++G(d,p). Theoretical and experimental UV-Visible investigation is correlated to obtain better insights into the absorption spectral studies. The experimental vibrational frequencies were compared with the scaled vibrational frequencies for the assignment of vibrational bands. Molecular electrostatic surface potential and Mulliken atomic charges are employed for the determination of charge density and reactive sites. In addition, the more precise computation of Mulliken atomic charges is done by comparing 6-311++G(d,p) and 6-311G(d,p) basis sets.

Graphical abstract

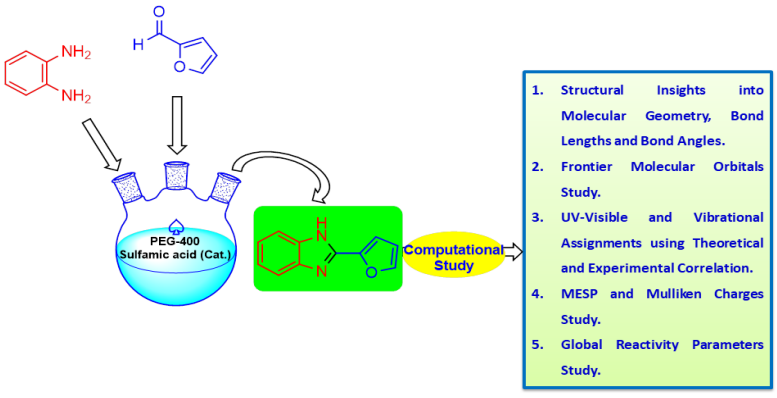

Keywords

DFT
2-(Furan-2-yl)-1*H*-benzo[*d*]imidazole
HOMO-LUMO
Molecular electrostatic surface potential

Article history

Received 03 May 2021
Revised 30 Aug 2021
Accepted 12 Nov 2021
Available online day month year

Handling Editor: Arlan Gonçalves

1. Introduction

Different molecular properties can be estimated using density functional theory (DFT). DFT is a computational quantum mechanical tool for studying the electronic structure of molecules that is used in chemistry and material science.

[a] Department of Chemistry, Mahatma Gandhi Vidyamandir's LVH Arts, Science and Commerce College, Panchavati, District- Nashik, India-422 003. (Affiliated to Savitribai Phule Pune University, Pune (MH), India). [b] Department of Chemistry, Mahant Jamanadas Maharaj Arts, Commerce and Science College, Karanjali, Taluka-Peth, District- Nashik, India-422 208. (Affiliated to Savitribai Phule Pune University, Pune (MH), India). Corresponding author. E-mail: **vishnuadole86@gmail.com**

DFT allows for a number of spectroscopic investigations, including: NMR chemical shifts, IR, UV-visible spectra, Raman spectra, and spin-spin coupling constants [1-5]. DFT calculations predict FMO energies, bond lengths, bond angles, dihedral angles, absorption energies, etc [6,7]. As theoretical calculations are compared to experimental findings, a lot of insights are achieved. Importantly, computation forecasts based on DFT make it possible to investigate reaction mechanisms [8,9]. The DFT methods are used to explore molecular, electronic, and spectroscopic properties of molecules like 2-acetoxybenzoic acid [10], thiophene-2-carbohydrazide [11], trans-4-hydroxy-L-proline [12], 2-arylidene indanones [13], fluconazole [14], 3-Ethoxy-4-hydroxy benzaldehyde [15], 7-chloro-1 methyl-5-phenyl-1,5-dihydro-benzo [1,4], diazepine-2,4-dione [16], sunitinib [17], -hydroxy-3-methoxycinnamaldehyde [18], (3,5-Diphenyl-4, 5-dihydro-1H-pyrazol-1-yl)(phenyl) methanone [19], etc.

Benzimidazole derivatives have pulled in tremendous attraction due their medicinal significances [20-25]. The excellent pharmacological profile benzimidazoles include properties like antibacterial [26], antifungal [27], anticancer [28], antitubercular [29], antiviral [30], antioxidant [31], anticonvulsant [32], anti-inflammatory [33], antihypertensive [34], antidiabetic [35], etc. These diverse biological properties of the benzimidazole derivatives have boosted many researchers to synthesize variety of benzimidazole scaffolds with promising biological activities. All these discussed facets energized us to synthesize and explore 2-(furan-2-yl)-1H-benzo[d]imidazole by using DFT method. Taking into account all these talked about imperative parts of the cutting edge times, in this, we wish to report theoretical study on molecular structure, electronic properties and chemical reactivity of 2-(furan-2-yl)-1H-benzo[d]imidazole. In the current research, DFT examination on molecular structure, bond length, bond angle, and Mulliken atomic charges have been explored. The important parameters such as total energy, HOMO-LUMO energies, charge distribution, thermodynamic properties, etc. also studied using the DFT method.

2. Results and Discussion

2.1 Computational Study

2.1.1 Molecular structure, bond length and bond angle study

The optimized molecular structure of 2-FBI obtained using DFT/B3LYP method with6-311++G(d,p) level is depicted in **Fig. 1**. The structural investigation infers that **2-FBI** is having C1 point group symmetry and dipole moment of 3.07 Debye. The E(RB3LYP) of titled compound is -608.87 a.u. The geometrical parameters, bond length and bond angle data of **2-FBI** is given in **Table 1** and **Table 2** respectively. The bond length data furnished in **Table 1** infers that the C1-C2 is the longest bond amongst all C=C bonds of benzene ring with a bond length value of 1.4166 Å. While the shortest bond in the benzene ring is C3-C4 with 1.3912 Å bond length distance. The C=C bond lengths in furan ring are C15-C16 and C18-C20 with 1.3655 Å and 1.3599 Å bond distance values respectively. The C7-C15 and C16-18 bonds have acquired double bond character and having 1.4424 Å and 1.429 Å bond distances respectively. The C2-N12bond has also acquired partial double bond nature with bond distance of 1.382 Å. The C-H bond lengths in 2-FBI are found to be approximately 1.08 Å long. The N12-H13 bond is 1.0077 Å long. Amongst carbon-nitrogen bonds C1-N14 is the longest with bond length value of 1.3826 Å. Both the pyrrole and furan ring structures have almost identical C-X-C bond angles. The bond angles for C15-O17-C20, C1-N14-C7, and C2-N12-C7 are respectively 106.9423°, 105.1312°, and 106.9447°. The benzimidazole and furan moieties are linked by the C7-C15 bond, which forms two essential bond angles: N14-C7-C15 and N12-C7-N15, which correspond to 125.3765° and 121.6807°, respectively. All other bond angles are perfect matches for the title molecule's structure.

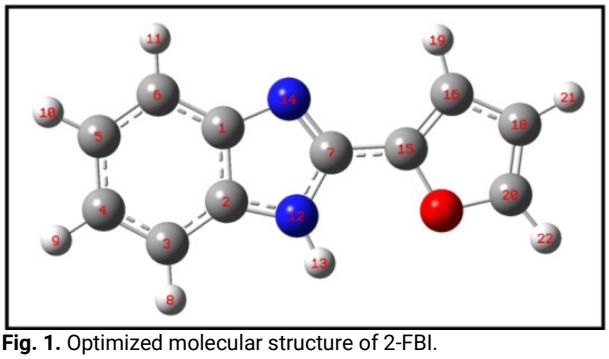

Fig. 1. Optimized molecular structure of 2-FBI.

Table 1. Bond lengths of 2-FBI.

Bond length (Å)			
C1- C2	1.4166	C7-N12	1.3806
C1-C6	1.3998	C7-N14	1.3144
C1-N14	1.3826	C7-C15	1.4424
C2-C3	1.3938	N12-H13	1.0077
C2-N12	1.382	C15-C16	1.3655
C3-C4	1.3912	C15-O17	1.3719
C3-C8	1.084	C16-C18	1.429
C4-C5	1.4082	C16-H19	1.0775
C4-H9	1.0839	O17-C20	1.3642
C5-C6	1.3887	C18-C20	1.3599
C5-H10	1.084	C18-H21	1.0783
C6-H11	1.0834	C20-H22	1.0766

Table 2. Bond angle of 2-FBI.

Bond Angle (°)			
C2-C1-C6	119.7327	N12-C7-N15	121.6807
C2-C1-N14	110.3871	N14-C7-C15	125.3765
C6-C1-N14	129.8802	C2-N12-C7	106.9447
C1-C2-C3	122.4922	C2-N12-H13	127.7299
C1-C2-N12	104.5941	C7-N12-H13	125.3254
C3-C2-N12	132.9137	C1-N14-C7	105.1312
C2-C3-C4	116.7784	C7-C15-C16	133.1772
C2-C3-H8	121.99	C7-C15-O17	116.8683
C4-C3-H8	121.2316	C16-C15-O17	109.9545
C-C4-C-5	121.4949	C15-C16-C18	106.2687
C3-C4-H9	119.2421	C15-C16-H19	125.4945
C5-C4-H9	119.2631	C18-C16-H19	128.2367
C4-C5-C6	121.4603	C15-O17-C20	106.9423
C4-C5-H10	119.0085	C16-C18-C20	106.5334
C6-C5-H10	119.5312	C16-C18-H21	127.2681
C1-C6-C5	118.0416	C20-C18-H21	126.1985
C1-C6-H11	120.2324	O17-C20-C18	110.3011
C5-C6-H11	121.726	O17-C20-H22	115.8758
C12-C7-N14	112.9428	O18-C20-H22	133.823

2.1.2 Frontier molecular orbital and UV spectral study

Fig. 2 depicts the FMOs; HOMO and LUMO pictorial representations. The HOMO energy is -5.89 eV, while the LUMO energy is -1.53 eV. The calculated HOMO-LUMO energy gap is found to be 4.36 eV on this basis. **Fig. 3** and **Fig. 4** demonstrate the theoretical and experimental electronic absorption spectra of the title compound. The theoretical spectra were simulated in gas phase, DCM, and

benzene solvents based on the experimental UV spectra recorded in DCM and benzene. The theoretical and experimental electronic absorption data is presented in **Table 3**. The gas phase electron absorption results showed the absorption maxima at 301.49 nm. On the other hand, theoretical UV-Visible simulations were found at 301.49 nm and 312.09 nm. This clearly indicates occurrence of blue shift while going from benzene to DCM solvent. The HOMO-LUMO transition is expressed by the configuration 48 -> 49. In all three phases, the oscillator strength is nearly identical. As compared to the experimental results for electronic absorptions, it indicates a higher level of agreement. UV absorption maxima in DCM and benzene were observed at 321.67 and 323.25 nm, respectively.

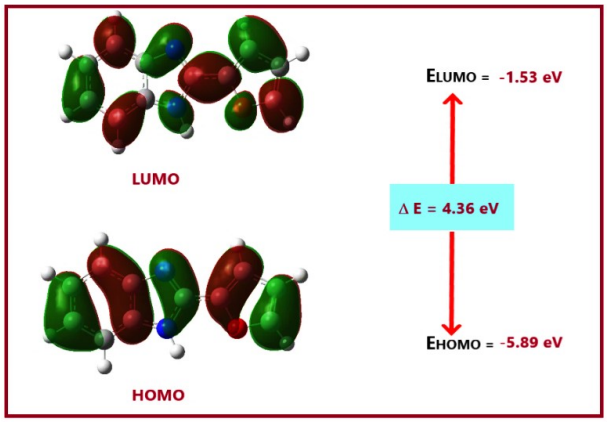

Fig. 2. The HOMO and LUMO plots by DFT/B3LYP method with 6-311G++G(d,p) basis set.

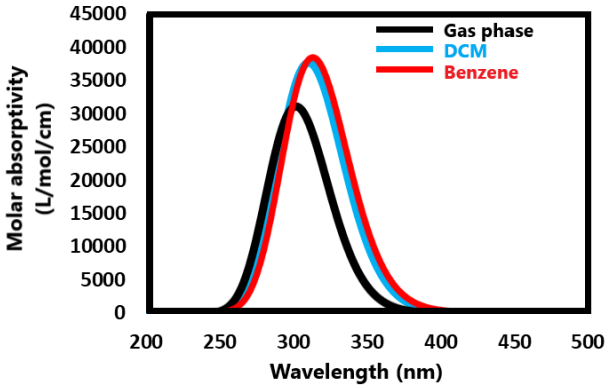

Fig. 3. Theoretical UV spectra in Gas phase, DCM and Benzene by DFT/B3LYP method with 6-311G++G(d,p) basis set.

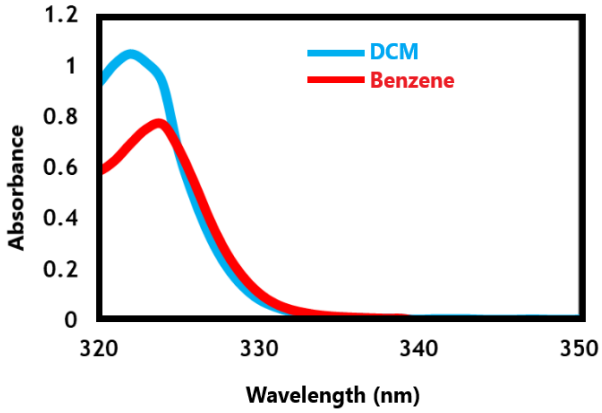

Fig. 4 Experimental UV spectra in DCM and Benzene.

Table 3. Theoretical and experimental electronic absorption data.

Type	Configuration	Oscillator strength	Wavelength (nm)	Excitation Energy
Theoretical Gas phase	48 -> 49	0.69427	301.49	4.11
Theoretical DCM	48 -> 49	0.69910	310.34	3.99
Theoretical Benzene	48 -> 49	0.69935	312.09	3.97
Experimental DCM	48 -> 49	-	321.67	3.73
Experimental Benzene	48 -> 49	-	323.25	3.71

2.1.3 Vibrational assignments and thermodynamic properties

The 2-(furan-2-yl)-1*H*-benzo[*d*]imidazole (2-FBI) molecule has 60 normal vibrational modes due to its 22 atoms. The vibrational spectral assignments were accomplished employing normal coordinate analysis. **Fig. 5–6** demonstrate the observed and simulated FT-IR spectra of **2-FBI**, respectively, for visual comparison. On the basis of the unscaled frequencies, a tentative assignment is frequently made by assuming that the observed frequencies are in the same order as the calculated ones. The calculated frequencies are then scaled by the scaling factor 0.96 to minimise the overall deviation for easier comparison to the observed values. **Table 4** displays the detailed vibrational assignments of **2-FBI's** fundamental modes. **Table 4** incorporates the corresponding experimental data. The scaled vibrational wavenumbers and theoretical IR intensities are also addressed. The title compound includes N-H, C=N, C=C, etc. as distinct functional groups to be observed in IR spectrum. The N-H peaks are usually observed at 3300-3500 cm^{-1}. The title compound has displayed a characteristic peak at 3379.29 cm^{-1} due to N-H stretching vibrations. The similar peak in the theoretical IR spectrum is found at 3509.43 cm^{-1}. The presence or absence of hydrogen bonding effect is due to the significant difference in the theoretical and experimental N-H vibrational peak. Since the titled compound is supposed to exhibit hydrogen bonding, which is not taken into account in theoretical simulations, the experimental IR value has been moved to the lower value. In the experimental FT-IR spectrum, the asymmetric stretching vibration of the C3-H-C6-H bond is found at 3059.10 cm^{-1}, which matches the scaled value of 3060.16 cm^{-1}. The experimental wavenumber at 1602.85 cm^{-1} correlating to the theoretical wavenumber at 1599.12 cm^{-1} is assigned to stretching vibrations of C7=C15 and C14=N7 bonds. Similarly, the stretching vibrations that are observed around 1350-1450 cm^{-1} are assigned to C15=C16, C1=C2, C15=C16, etc. The *in*-plane bending modes of Ph-H and furan-H are observed at 1274.95 and 1165.00 respectively and ideally matches with the theoretical values. The deformation modes of benzimidazole and furan ring are located at 736.81 cm^{-1} and 584.43 cm^{-1} respectively correlates with 736.76 cm^{-1} and 603.49 cm^{-1} in theoretical spectrum. Out-of-plane and scissoring modes are two other significant bands seen in the experimental IR spectrum. In conclusion, there is a great deal of correlation between the experimental and scaled vibrational wavenumbers, which

enabled assignment of different modes of vibration in an easiest way in the **2-FBI**.

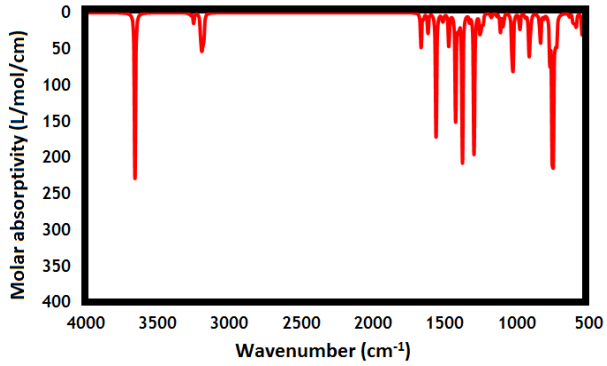

Fig. 5. Theoretical IR spectrum (unscaled) of the title compound obtained at 6-311++G (d,p) as basis set.

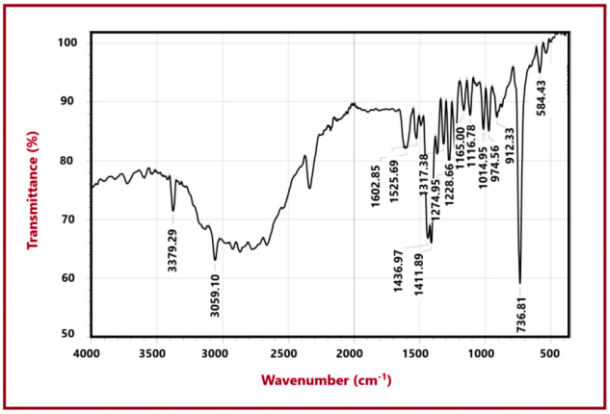

Fig. 6. Experimental IR spectrum of the title compound obtained on Shimadzu FTIR.

Table 4. Selected experimental and theoretical vibrational assignments calculated at B3LYP/6-311++G(d,p) level.

Mode	Computed scaled frequencies (cm^{-1})	IR Intensity (km) mol^{-1}	Experimental frequencies (cm^{-1})	Assignment
60	3509.43*	66.78	3379.29	*v* N-H
55	3060.16	19.11	3059.10	asym C3-H-C6-H
52	1599.12	14.64	1602.85	*v* C7=C15 and *v* C14=N7
49	1497.84	49.63	1525.69	*v* C20=C18
47	1449.03	3.30	1436.97	*v* C15=C16
46	1411.49	15.30	1411.89	*v* C1=C2
43	1322.22	65.87	1317.38	*v* C5=C6
42	1273.82	3.01	1274.95	β Ph-C-H
41	1243.04	59.73	1228.66	*v* C1-N14
38	1186.19	7.63	1165.00	β furan ring C-H
36	1123.62	0.85	1116.78	Scis C4-H-C5-H
34	1068.74	8.25	1074.56	β N-H and def furan ring
31	984.29	22.76	974.05	β furan ring C-H and β Ph-C-H
28	901.50	2.32	912.33	γ Ph-C-H
20	736.76	17.39	736.81	def benzimidazole ring
14	603.49	6.72	584.43	def furan ring

v-stretching; sym-symmetric; asym-asymmetric; def-deformation; β-in-plane bending; γ-out of plane bending

**The theoretical simulation is devoid of intra/intermolecular hydrogen bonding, which could be present in the experimental results, so the simulated scaled wavenumber is higher than the experimental wavenumber.*

2.1.4 Molecular electrostatic surface potential and Mulliken atomic charges study

The study of the association between molecular structures and their physiochemical property relationships, like biomolecules and drugs, has found that molecular electrostatic potential is a very useful method. **Fig. 7** shows the total electron density mapped with the molecular electrostatic potential surface (MESP) and the contour plot for the **2-FBI** molecule at the B3LYP/6-311++G(d,p) basis set. The MESP is a useful property to study reactivity. The different electrostatic potential values of the surface are expressed by different colors, with the most negative area, which is the favored location for electrophilic reactivity, being shown in red and yellow. In terms of colour grading, MESP is important because it simultaneously shows molecular size, form, as well as positive, negative, and neutral electrostatic potential regions. The eventual plot indicates molecular size, shape, and electrostatic potential value all at once. Potential augments in the ascending sense: red, orange, yellow, green and blue. The maximum positive region, which is the desired site for nucleophilic reactivity, is shown as a blue region in the MESP plot of the **2-FBI** molecule, while green represents zero potential. The computed outcome of the study demonstrates that negative potentials are primarily over electronegative nitrogen and oxygen atoms, whereas positive potentials are primarily over the nucleophilic reactive hydrogen atom attached to the nitrogen atom. This finding also reveals the area in which the titled compound is capable of intermolecular interaction. The contour map makes it easy to predict how various geometries will respond.

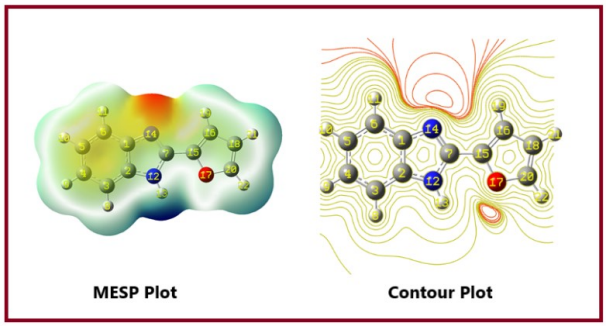

Fig. 7. Molecular electrostatic potentials by DFT/B3LYP method with the 6-311++G (d,p) as basis set.

Mulliken atomic charges influence dipole moment, polarizability, electronic structure, and many other properties

of molecular structures, Mulliken atomic charge measurement plays an essential part in applying quantum chemical calculations to them. The dipole moment, electronic parameters, polarizability, and refractivity are all supposed to be affected by these charges. The atomic charges were determined using the Mulliken population analysis of the title compound at the B3LYP/6-311++G(d,p) and B3LYP/6-311G(d,p) stage. Mulliken charges differs a lot based on the basis set, so the Mulliken population was done for both higher and lower basis sets. Mulliken charges, in general, exhibit basis set dependency, which is always very high. **Table 6** shows the charge distributions determined using the Mulliken process for the optimized geometry of **2-FBI**. The graphical representation of the data is given in **Fig. 8** and used for visual comparison. In a 6311++G(d,p) base set, the N12, N14, and O17 have -0.283814e, -0.066309e, and -0.041845e Mulliken charges respectively. In the 6311G(d,p) basis set, the Mulliken charge values for these atoms are -0.465441e, -0.349305e, and -0.287940e, respectively. The electronegative atoms are usually found to exhibit more negative values of Mulliken atomic charges. As a result, it could be concluded here, the Mulliken population for these three electronegative atoms is best obtained using the lower basis set rather than the higher basis set. The C6 carbon atom has -0.476350e Mulliken atomic charge value in 6311++G(d,p) basis set and is the highest in terms of negative value. The same atom has -0.068670e Mulliken atomic charge value 6311G(d,p) basis set. Since the C7 carbon is flanked by two electronegative nitrogen atoms, a significant positive value of Mulliken atomic charge is anticipated. The 6311G(d,p) basis set has provided a more positive Mulliken atomic charge value of 0.356233e for the C7 atom. When using the 6311++G(d,p) base set, the C2 atom (attached to just one nitrogen atom) has a higher positive Mulliken atomic charge value. This explicitly demonstrates that a larger basis set would not imply more accurate outcomes.

Table 5. Mullikan atomic charges.

6311++G(d,p)				6311G(d,p)			
1 C	0.168416	12 N	-0.283814	1 C	-0.013060	12 N	-0.465441
2 C	0.573609	13 H	0.332772	2 C	0.196900	13 H	0.237576
3 C	-0.564746	14 N	-0.066309	3 C	-0.053749	14 N	-0.349305
4 C	-0.143176	15 C	-0.190293	4 C	-0.110993	15 C	0.113759
5 C	-0.315347	16 C	-0.058307	5 C	-0.104856	16 C	-0.064054
6 C	-0.476350	17 O	-0.041845	6 C	-0.068670	17 O	-0.287940
7 C	0.116634	18 C	-0.385451	7 C	0.356233	18 C	-0.162603
8 H	0.141080	19 H	0.205556	8 H	0.088060	19 H	0.110041
9 H	0.167369	20 C	0.131691	9 H	0.092811	20 C	0.078987
10 H	0.158718	21 H	0.174306	10 H	0.092313	21 H	0.108234
11 H	0.173890	22 H	0.181599	11 H	0.095533	22 H	0.110225

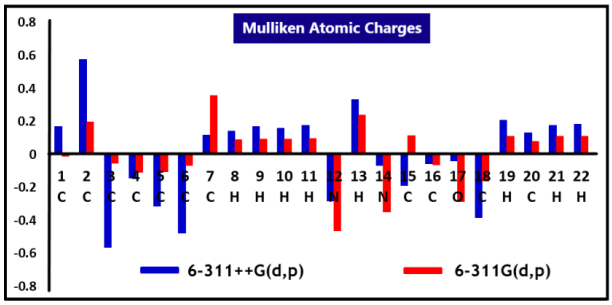

Fig. 8. Graphical representation of Mulliken population analysis.

3. Material and Methods

3.1 General Remarks

The chemicals (Make- SD Fine Pvt. Ltd., and Avra synthesis) with high purity were purchased from Sigma laboratory, Nashik, and used as received. The FT-IR spectrum of the title compound was recorded on Shimadzu spectrometer using a KBr disc technique. The NMR experiment was performed on a sophisticated multinuclear FT-NMR Spectrometer (500 MHz) model Advance-II (Bruker). The compound was dissolved in DMSO-d6 and the chemical shifts were reported in ppm relative to tetramethylsilane. The reaction was followed by using thin-layer chromatography on Merck Aluminium TLC plate, silica gel coated with fluorescent indicator F254. All the glass apparatus were cleaned and dried in the oven prior to use.

3.2 Experimental Procedure for the Synthesis of 2-(furan-2-yl)-1*H*-benzo[*d*]imidazole

In a 50 mL flat bottom flask already containing 20 mL PEG-400 solvent, equimolar amount of o-phenylenediamine (**1**, 0.01 mol) and furfural (**2**, 0.01 mol) were mixed. The mixture was stirred at 70-80 ℃ until dissolution of o-phenylenediamine. After this step, catalytic amount of sulfamic acid was added and stirring with heating was continued until the formation of the product. Then, the reaction mixture was poured into crushed ice. The product was filtered, washed, dried, and recrystallized. The formation of 2-(furan-2-yl)-1*H*-benzo[*d*]imidazole is depicted in **Scheme 1**.

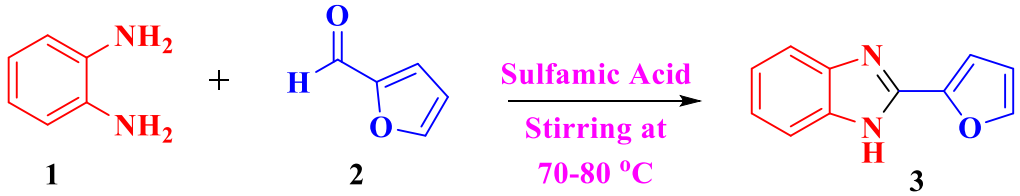

Scheme 1. Formation of 2-FBI.

3.3 Computational Details

For DFT calculations Gaussian 03(W) program package was used. All the calculations were performed at optimized by using DFT/B3LYP method using 6-311++G(d,p) basis set. Gauss View 4.1 molecular visualization program was used to visualize the optimized structure. The structural parameters like bond length and bond angles, Mulliken atomic charges, molecular electrostatic surface potential, and thermochemical data for the title compound were determined. All the DFT calculations were performed for the optimized molecular structure in the gas phase.

3.4 Spectral Analysis

2-(Furan-2-yl)-1*H*-benzo[*d*]imidazole: Yield-80%; Pale yellow solid; m.p. 282-284 °C; FT-IR (KBr): cm^{-1} 3379.29 3059.10 1602.85 1525.69 1436.97 1411.89 1317.38 1274.95 1228.66 1165.00 1116.78 1014.56 974.05; ^{1}H NMR (500 MHz, DMSO-d6) δ (ppm) 12.93 (s, 1H), 7.95 (dd, 1H), 7.63 (d, 1H), 7.50 (d, 1H), 7.25 – 7.16 (m, 3H), 6.74 (dd, 1H); ^{13}C NMR (126 MHz, DMSO-d6) δ (ppm) 146.03, 145.11, 144.10, 134.69, 123.10, 122.27, 119.24, 112.80, 111.81, 110.94.

4. Conclusions

In this research, 2-(furan-2-yl)-1H-benzo[d]imidazole (2-FBI) was synthesized and investigated using computational chemistry. The computational calculations were carried out using the density functional theory (DFT) method, with a basis set of 6-311++G. (d,p). The structure of 2-FBI was established using FT-IR, ^{1}H NMR, and ^{13}C NMR spectroscopic methods. The FMO study revealed the HOMO-LUMO energy gap of 4.36 eV. Based on experimental UV spectra recorded in DCM and benzene, theoretical spectra were simulated in gas phase, DCM, and benzene solvents. When switching from benzene to DCM solvent, a blue shift is taking place in the titled compound. The experimental and scaled vibrational wavenumbers have a high degree of correlation, allowing for simple assigning of various modes of vibration. The MESP study infers that the negative potentials are mainly over electronegative nitrogen and oxygen atoms, while positive potentials are primarily over the nucleophilic reactive hydrogen atom bound to the nitrogen atom. The atomic charges of the title compound were calculated using Mulliken population analysis at the B3LYP/6-311++G(d,p) and B3LYP/6-311G(d,p) levels. It has been established that a lower basis set is superior to a higher basis set for the analysis of Mulliken atomic charges. In conclusion, the study presented in the present research would be helpful for the researchers working in the field of computational chemistry.

Acknowledgments

Authors acknowledge central instrumentation facility, Savitribai Phule Pune University. Authors also would like to thank LVH Arts, Science and Commerce College for permission and providing necessary research facilities. Prof. Dr. A. B. Sawant and Prof. Dr. T. B. Pawar are acknowledged for the DFT study. Dr. Aapoorva P. Hiray, Coordinator, MG Vidyamandir Institute, is gratefully acknowledged for Gaussian package.

Author Contributions

Conceptualization, V.A.A. and R.H.W; Methodology, S V.A.A. and R.H.W.; Investigation, B.S.J.; Writing – Original Draft, V.A.A.; Writing – Review & Editing, V.A.A. and R.H.W.; Resources, V.A.A. and R.H.W.; Supervision, B.S.J.

References and Notes

[1] Pierens, G. K. *J. Comput. Chem.* **2014**, *35*, 1388. [Crossref]

[2] Pathade, S. S.; Jagdale, B. S. *Phys. Chem. Res*. **2020**, *8*, 671. [Crossref]

[3] Adole, V. A.; Pawar, T. B.; Jagdale, B. S. *J. Sulphur Chem.* **2020**, *42*, 131. [Crossref]

[4] Madhavan, V. S.; Varghese, H. T.; Mathew, S.; Vinsova, J.; Panicker, C. Y. Spectrochim. *Acta A Mol. Biomol. Spectrosc.* **2009**, *72*, 547. [Crossref]

[5] Malkin, V. G.; Malkina, O. L.; Salahub, D. R. *Chem. Phys. Lett.* **1994**, *221*, 91. [Crossref]

[6] Pathade, S. S.; Adole, V. A.; Jagdale, B. S.; Pawar, T. B. *Curr. Res. Green Sustain. Chem.* **2021**, *4*, 100172. [Crossref]

[7] Rouhani, M. *J. Mol. Struct.* **2018**, *1173*, 679. [Crossref]

[8] Rhyman, L.; Ramasami, P.; Joule, J. A.; Sáez, J. A.; Domingo, L. R. *RSC Adv.* **2013**, *3*, 447. [Crossref]

[9] Domingo, L. R.; Sáez, J. A.; Joule, J. A.; Rhyman, L., Ramasami, P. *J. Org. Chem*. **2013**, *78*, 1621. [Crossref]

[10] Govindasamy, P.; Gunasekaran, S.; Srinivasan, S. *Spectrochim. Acta A Mol. Biomol. Spectrosc.* **2014**, *130*, 329. [Crossref]

[11] Balachandran, V.; Janaki, A.; Nataraj, A. *Spectrochim. Acta A Mol. Biomol. Spectrosc*. **2014**, *118*, 321. [Crossref]

[12] Xavier, R. J.; Dinesh, P. *Spectrochim. Acta A Mol. Biomol. Spectrosc.* **2014**, *128*, 54. [Crossref]

[13] Adole, V. A.; Jagdale, B. S.; Pawar, T. B.; Sawant, A. B. *J. Chin. Chem. Soc.* **2020**, *67*, 1763. [Crossref]

[14] Chandrasekaran, K.; Kumar, R. T. *Spectrochim. Acta A Mol. Biomol. Spectrosc.* **2015**, *150*, 974. [Crossref]

[15] Chithambarathanu, T.; Vanaja, K.; Magdaline, J. D. *Rasayan J. Chem*. **2015**, *8*, 490.

[16] Sylaja, B.; Gunasegaram, S.; Srinivasan, S. *Optik* **2016**, *127*, 5055. [Crossref]

[17] Mıhçıokur, Ö.; Özpozan, T. *J. Mol. Struct.* **2017**, *1149*, 27. [Crossref]

[18] Thirunavukkarasu, K.; Rajkumar, P.; Selvaraj, S.; Suganya, R.; Kesavan, M.; Gunasekaran, S.; Kumaresan, S. *J. Mol. Struct.* **2018**, *1173*, 307. [Crossref]

[19] Dhonnar, S. L.; Adole, V. A.; Sadgir, N. V.; Jagdale, B. S. *Phys. Chem. Res.* **2019**, *9*, 193. [Crossref]

[20] Rajasekhar, S.; Maiti, B.; M Balamurali, M.; Chanda, K. *Curr. Org. Synth.* **2017**, *14*, 40. [Crossref]

[21] Babbar, R.; Arora, S. A. *J. Pharm. Technol. Res. Manag*. **2020**, *8*, 23. [Crossref]

[22] Vasava, M. S.; Bhoi, M. N.; Rathwa, S. K.; Jethava, D. J.; Acharya, P. T.; Patel, D. B.; Patel, H. D. *Mini Rev. Med. Chem*. **2020**, *20*, 532. [Crossref]

[23] Bansal, Y.; Silakari, O. *Bioorg. Med. Chem*. **2012**, *20*, 6208. [Crossref]

[24] Yadav, S.; Narasimhan, B. *Anticancer Agents Med. Chem*. **2016**, *16*, 1403. [Crossref]

[25] Boiani, M.; González, M. *Mini Rev. Med. Chem*. **2005**, *5*, 409. [Crossref]

[26] He, Y.; Yang, J.; Wu, B.; Risen, L.; Swayze, E. E. *Bioorg. Med. Chem. Lett*. **2004**, *14*, 1217. [Crossref]

[27] Vargas-Oviedo, D.; Butassi, E.; Zacchino, S.; Portilla, J. *Monatsh. Chem*. **2020**, *151*, 575. [Crossref]

[28] Shaharyar, M.; Abdullah, M. M.; Bakht, M. A.; Majeed, J. *Eur. J. Med. Chem*. **2010**, *45*, 114. [Crossref]

[29] Kumar, K.; Awasthi, D.; Lee, S. Y.; Zanardi, I.; Ruzsicska, B.; Knudson, S.; Tonge, P. J.; Slayden, R. A.; Ojima, I. *J. Med. Chem.* **2011**, *54*, 374. [Crossref]

[30] Tonelli, M.; Simone, M.; Tasso, B.; Novelli, F.; Boido, V.; Sparatore, F.; Paglietti, G.; Pricl, S.; Giliberti, G.; Blois, S.; Ibba, C. *Bioorg. Med. Chem*. **2010**, *18*, 2937. [Crossref]

[31] Tonelli, M.; Simone, M.; Tasso, B.; Novelli, F.; Boido, V.; Sparatore, F.; Paglietti, G.; Pricl, S.; Giliberti, G.; Blois, S.; Ibba, C. *Bioorg. Med. Chem*. **2010**, *18*, 2937. [Crossref]

[32] Siddiqui, N.; Alam, M. S.; Ali, R.; Yar, M. S.; Alam, O. *Med. Chem. Res.* **2016**, *25*, 1390. [Crossref]

[33] Achar, K. C.; Hosamani, K. M.; Seetharamareddy, H. R. *Eur. J. Med. Chem*. **2010**, *45*, 2048. [Crossref]

[34] Jain, A.; Sharma, R.; Chaturvedi, S. C. *Med. Chem. Res*. **2013**, *22*, 4622. [Crossref]

[35] Shingalapur, R. V.; Hosamani, K. M.; Keri, R. S.; Hugar, M. H. *Eur. J. Med. Chem.* **2010**, *45*, 1753. [Crossref]

How to cite this article

Adole, V. A.; Jagdale, B. S.; Waghchaure, R. H. *Orbital: Electron. J. Chem.* **2021**, *13*, 413. DOI: http://dx.doi.org/10.17807/orbital.v13i5.1625